

Short Communication

Creep behavior of 316 austenitic stainless steel under variant operating conditions

Mohammad Sajjadnejad^{a,*} , Seyyed Mohammad Saleh Haghshenas^b, Mina Tavangar^a, Azin Niloofer Ghani Kolahloo^a

^a Department of Materials Engineering, School of Engineering, Yasouj University, Yasouj, Iran

^b Department of Materials Science and Engineering, School of Engineering, Shiraz University, Shiraz, Iran

ARTICLE INFORMATION

Received: 13 February 2020
Received in revised: 14 April 2020
Accepted: 18 April 2020
Available online: 4 June 2020

DOI: 10.26655/AJNANOMAT.2020.4.1

KEYWORDS

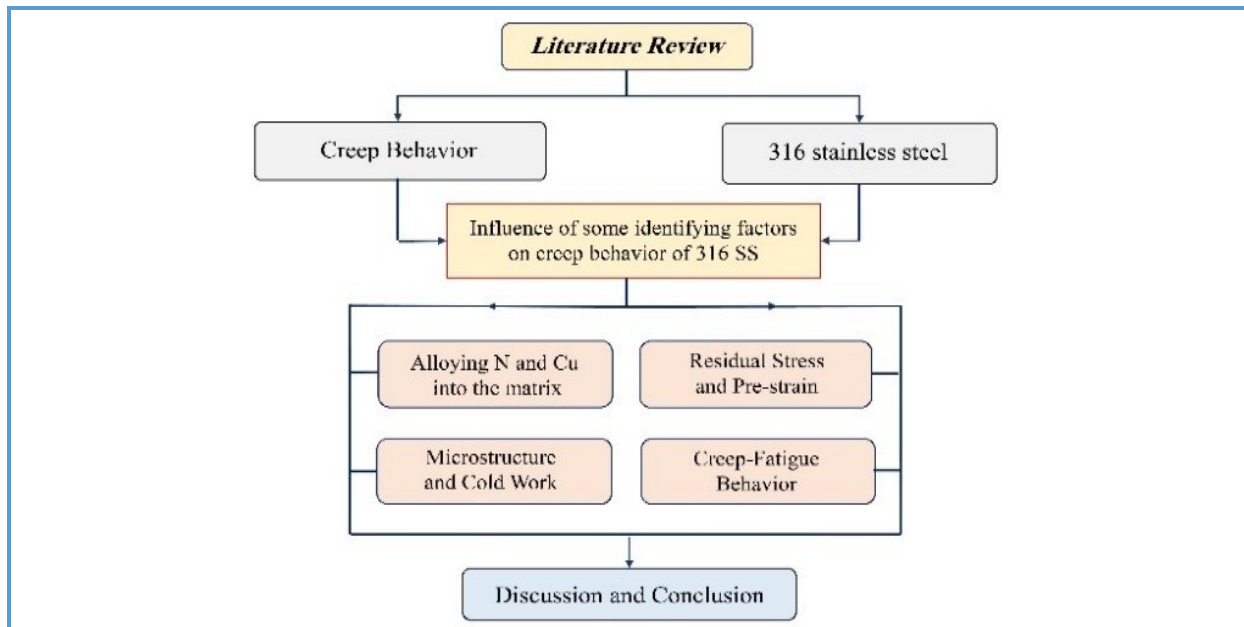
Creep
AISI 316 stainless steel
Residual stress
Microstructure
Creep-fatigue

ABSTRACT

Creep behavior of AISI 316 austenitic stainless steel as one of the most fundamental materials utilized in high temperature operating conditions due to their good high-temperature mechanical properties in various industries such as high temperature power generation plants, gas and steam turbines, pipelines, weld joints, pressure vessels, and heat exchangers. This review attempted to cover some identifying factors on the creep behavior of the 316 stainless steel such as addition of alloying elements such as N and Cu into the matrix, presence of residual stress and pre-strain, microstructure and cold work. In addition, the creep-fatigue combination behavior of the 316 austenitic stainless steel was discussed.

© 2020 by SPC (Sami Publishing Company), Asian Journal of Nanoscience and Materials, Reproduction is permitted for noncommercial purposes.

Graphical Abstract



Biographies



Mohammad Sajjadnejad He received her M.Sc in Materials Science and Engineering in the area of Corrosion Engineering from Sharif University of Technology, Tehran, Iran in 2011. Then he received his PhD in Materials Science and Engineering in the area of Surface and Electrochemical Engineering from Amirkabir University of Technology (Tehran Polytechnic), Tehran, Iran in 2015. He has been working as an Assistant Professor of Materials Science and Engineering since 2015 after PhD graduation. His research encompasses surface, corrosion and electrochemical engineering.



Seyyed Mohammad Saleh Haghsheenas He received his B.Sc. in Materials Science and Engineering from Shiraz University (Iran), in 2015 and M.Sc in Corrosion and Protection of Materials from Shiraz University (Iran), in 2018. His research encompasses Corrosion, Coatings and Surface Science, Metallurgical and Mechanical Aspects of Materials, Advanced Materials, and Composites.



Mina Tavangar She received her B.Sc in Materials Engineering (Ceramics Technology) from Azad University (Iran), in 2015 and her M.Sc in Selection and Identification of Engineering Materials from Yasuj University (Iran), in 2019. Her research encompasses the manufacturing, characterization and evaluation of bio-scaffolds, bone glue and nanocomposite.



Niloofar Ghani Kolahloo She received her B.Sc in Materials Engineering from Shahid Bahonar University (Iran), in 2015 and her M.Sc in Selection and Identification of Engineering Materials from Yasuj University (Iran), in 2019. Her research encompasses the synthesis of spinels and investigation of the mechanochemical process.

Table of Contents

Introduction

Effect of Different Factors on Creep Behavior of 316 L SS

Effect of addition of N and Cu

Effect of residual stress and pre-strain

Effect of microstructure and cold work

Creep-fatigue combination behavior

Conclusions

Disclosure Statement

References

Abbreviations

Biographies

Graphical abstract

Orcid

Introduction

Creep is a time-dependent plastic deformation mechanism occurred at elevated temperatures. It has been considered as one of the most serious failure mechanisms in high-temperature power generation plants [1]. Stainless steels (SS) are widely used in power plants for components which operate at high temperatures [2]. For instance, reheat cracking in, and adjacent to, heat affected zones in thick-section stainless steel welds [3] has been associated with the relaxation of residual stresses acting as a driver for formation of the crack damage. It is presumed that the

conversion of elastic strain to creep strain during the residual stress relaxation may results in development of creep damage, acting as the precursor to the initiation of cracks [1].

316 stainless steels are the highly functional materials that can operate at high temperature environments with high temperature gradients, as those happening in aircraft gas turbine engine or hot section combustor liners [4], due to their good high-temperature mechanical properties [5, 6]. The 316 SS material has been utilized as an established material for elevated stresses and temperatures such as steam turbines, pressure vessels, piping, weld joints

and various power machineries and is prevalently exposed to asymmetrically proportional loading during service [6]. Moreover, the 316L SS has an oxidation resistance of up to 900 °C and a reasonable cost [7]. Long-term creep properties of the structural materials used in high-temperature plants are evaluated from short-term data with the aid of time-temperature-parameter (TTP) methods [8]. However, the conventional TTP methods sometimes overestimate long-term creep rupture life and the overestimation has been pointed out on austenitic stainless steels [9-11]. The conventional TTP methods are not capable of accurately describing the rupture data of the 316 stainless steel studied. The activation energy, Q , for the rupture life variations within a set of creep ruptures data, in contrast to the basic presumption of the conventional TTP methods. The Q variations stand for the poor fit of the conventional TTP method to the creep rupture data [12].

The 316 stainless steels operating at high-temperature applications, such as in gas turbine blades and hot section combustor liners. Low cycle fatigue (LCF) damages can be occurred due to the startup/shut-down cycling. Moreover, the high-temperature components are exposed to the time-dependent creep damage due to their normal operation at elevated temperatures during services [4]. Therefore, the creep-fatigue behavior needs special and in some cases complex investigation in order to assess the mechanisms [4, 6, 13, 14]. In the following, some identifying factors such as addition of N and Cu in to the matrix, residual stress and pre-strain, microstructure and cold work, and the creep-fatigue combination behavior of 316 austenitic stainless steel are discussed. The schematic flowchart of review is illustrated in Figure 1.

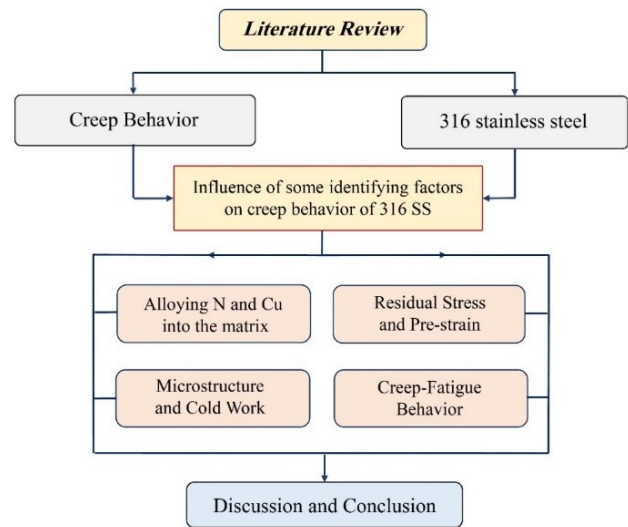


Figure 1. The schematic flowchart of review

Effect of Different Factors on Creep Behavior of 316 L SS

Effect of addition of N and Cu

For the high-temperature structural components, 316 L stainless steel with 0.02-0.03 wt.% carbon and 0.06-0.08 wt.% nitrogen is one of the preferred materials [15]. The carbon content is kept low to minimize the steel susceptibility to sensitization of the heat affected zone (HAZ) in welded components and thus the stress corrosion cracking potential of HAZ in a corrosive environment is deducted. Alloying with 0.06–0.08 wt.% nitrogen helps to increase the high temperature strength of 316 L SS to levels comparable to that of 316 SS [16]. Nitrogen is a strong austenite stabilizer, solid solution strengthener, and it can improve the pitting corrosion resistance of 316 L SS. Nitrogen is known to improve the creep and fatigue strength at high temperatures and fracture toughness at cryogenic temperatures. Nitrogen alloying into the matrix has led to improve properties which are reported in ferritic steels, austenitic steels, martensitic steels and duplex steels [15]. Mathew *et al.* in 1991 [17], investigated the influence of carbon

and nitrogen on the creep properties of type 316 stainless steel at 873 K. Their results indicated that type 316 LN SS at 873 K in the stress range 215-335 MPa, has a lower steady state creep rate compared to type 316 SS, higher creep rupture strength and higher rupture ductility. The improvement in creep properties has been ascribed to the combined effect of precipitation strengthening by fine intra-granular and inter-granular carbides and strengthening arising from the nitrogen in solid solution. Carbides in type 316 SS, precipitate on grain boundaries and subsequently on dislocations in the grains. Therefore, a decrease was observed in solid solution strengthening by carbon and an additional strengthening by precipitation. As the time goes on, carbides grow, leading to grain boundary embrittlement and decrease in precipitation strengthening with reduction in strength and ductility. On the contrary, in type 316 LN SS, solid solution strengthening by nitrogen and reduction in

carbides coarsening leads to higher ductility and strength.

Sasikala *et al.* in 2000 [5], investigated the creep properties of a 316 L SS doped with nitrogen (316 LN). Its weld metal was also studied at 873 and 923 K in the range of applied stresses from 100 MPa to 335 MPa. Details of the weld pads preparation and chemical compositions (in weight percent, wt.%) of the base and weld metals of 316 and 316 L(N) SS are presented in Tables 1 and 2. The results indicated that, the rupture lives of the weld metal were lower, by a factor of 5 to 10, compared to the respective base metals. The rupture elongations of the 316 L(N) SS base metal were similar to or higher than those for the 316 SS, whereas its weld metal showed clearly lower ductility than that of the 316 SS weld metal. The observed properties could be vindicated based on the distinction in precipitation kinetics of the two (316 L and 316 LN) steels and their welds and their influence on the properties [5].

Table 1. Details of the weld pads preparation [5]

Process	Shielded Metal Arc
Joint design	Single U groove
Number of passes	9
Interpass temperature	Less than 423 K
Flux	Basic coated
Current	150 A
Voltage	25 V
Travel speed	3 mm/s
Heat input rate	0.875 kJ/mm

Table 2. Chemical compositions (Wt.%) of the Base and Weld Metals of 316 and 316 L(N) SS [5]

Element	Base Metal		Weld Metal	
	316	316L(N)	316	316L(N)
C	0.048	0.023	0.060	0.052
Ni	12.48	12.21	11.9	11.5
Cr	16.10	17.12	18.8	18.6
Mo	2.11	2.31	2.06	2.20
Mn	1.73	1.65	1.42	1.74
Cu	0.225	0.10	0.05	0.04

Si	0.295	0.29	0.58	0.64
B	0.0005	0.0012	0.0005	0.0009
S	0.0016	0.003	0.010	0.007
P	0.03	0.024	0.010	0.022
N	0.031	0.086	-	0.067

The beneficial effects of nitrogen in austenitic stainless steels are many: (1) its solubility is much higher than that of carbon, (2) it reduces the stacking-fault energy of the matrix [18], and (3) it introduces strong elastic distortions into the crystal lattice, giving rise to strong solid solution hardening [19]. Alloying nitrogen leads to increase the tensile strength, creep and fatigue in austenitic stainless steel. Multiple reasons have been proposed for increasing the strength: (1) solid solution strengthening, (2) reduction in stacking fault energy, (3) sedimentation enhancement, (4) formation of interstitial-solute compounds, (5) clustering and (6) order strengthening [5, 15, 17, 20–22].

Mathew *et al.* in 2011 [15], reported that the addition of N was found to be beneficial to creep properties at all the stress levels and creep rupture strength increased substantially with increase in N content which led to increase in the creep rupture life. Creep rupture life increased almost 10 times by increasing nitrogen content from 0.07 wt.% to 0.22 wt.%. It also reduced the steady state creep rate and strain. All the three stages time elongation was enhanced with increasing the nitrogen content, giving rise to an overall enhancement in rupture life. Moreover, intergranular and surface cracks were reduced with increasing the nitrogen content. Also, nitrogen in $M_{23}C_6$ precipitates suppressed the mismatch between the precipitate and the austenite matrix thereby reducing the interfacial energy and inhibits precipitate coarsening. Nitrogen also reduces the diffusivity of carbon and chromium atoms and thus delays over-aging of the carbides. Such enhancement was ascribed to solid solution

strengthening which led to increase young's modulus, decrease in stacking fault energy and matrix precipitation strengthening of carbonitride precipitates led to increase in creep strength with increasing nitrogen incorporation [15].

The molten carbonate fuel cell (MCFC) is an absorption source for clean energy, which has a very important component called a dipole plate, which is often made of 316 L austenitic stainless steel. The 316 L steel has an oxidation resistance of up to 900 °C and a reasonable cost [7]. However, the in-service of this stainless steel is limited by its relatively low creep resistance, which is proposed to add N and Cu to 316 L stainless steel to improve the creep properties (while maintaining good oxidation resistance). The addition of nitrogen increases the failure time and decreases the creep and strain rate, which increases the elastic modulus. In fact, increasing the amount of N reduces the stacking fault energy [15].

Chi *et al.* in 2012 [23], investigated the addition of 2–3 wt.% Cu on 18Cr9Ni3CuNbN steel. Their results exhibited that Cu constantly diffuses and segregates to a small area (~1 nm) and gradually forms precipitates of a Cu-rich phase. The research results obtained by Bai *et al.* in 2013 [24], indicated that these particles remain small (~30 nm) even after aging for 104 h at 650 °C, surprisingly. Moreover it has led to enhance the mechanical properties including hardness [23, 25] as well as tensile strength [23] was ascribed to the Cu-rich phase precipitation. However, Sen *et al.* [26], asserted that the precipitation did not have noticeable influence on tensile properties, and grain growth causes the deduction in fatigue crack

growth after aging. Moreover, the precipitation of the Cu-rich phase is reported to be enhanced by deformation [27–29]. Thus, the precipitation is likely to be facilitated under stress and creep behavior would be improved. In the case of a 347 austenitic stainless steel, Cu improved the rupture life at 750 °C with a stress range of 70–120 MPa due to the precipitation of the Cu-rich phase [30].

Cai *et al.* in 2016 [31], investigated the addition of N and Cu in 316 L SS to improve the creep life by analyzing tensile strengths at 650 °C and 700 °C held under a stress range of 100–250 MPa. The investigated alloys chemical composition is reported in Table 3. An increased amount of N in solid solution strengthened the matrix and suppressed the coarsening of $M_{23}C_6$ precipitates, which improved the creep life. Low stresses allowed

Cu-added alloys to rupture after the precipitation of the Cu-rich phase, which strengthens the matrix. Therefore, the addition of Cu enhanced the creep life only under low stresses while the positive effect of Cu was not significant under high stresses. Therefore, both temperature and stress must be considered in order to use the beneficial effect of Cu precipitation in the matrix [31]. Adding nitrogen to a solid solution improves the yield stress and tensile strength, while the effect of copper on tensile strength is low. On the other hand, due to addition nitrogen to the alloys, the creep life rises significantly. The addition of copper can improve the creep life at low stress, due to the fine precipitation of the Cu-rich phase [27–29]. While the formation of copper-rich phase before the failure did not influenced the creep life under high stress.

Table 3. Chemical composition of alloys (wt.%). Fe is balanced

Alloy	C	Cr	Ni	Mo	Mn	N	Cu
5N	0.0205	18.68	9.17	2.05	1.06	0.0492	-
9N	0.0177	17.94	8.97	2.01	1.03	0.0877	-
13N	0.0176	17.93	9.06	1.99	1.01	0.1346	-
5N1Cu	0.0154	19.15	9.55	2.02	1.10	0.0397	0.98
5N2Cu	0.0172	19.25	9.73	2.07	1.11	0.0461	2.05

Effect of residual stress and pre-strain

If the accumulated creep strains are sufficient to use up the creep ductility, extensive grain boundary creep cavitation is developed and cracking is initiated. Creep damage is primarily associated with the residual stress relaxation which may cause the failure mode commonly referred to reheat cracking due to the development of cracking within welds or near regions during stress relief heat treatment [32].

Austenitic stainless steels have relatively poor resistance to intergranular stress corrosion cracking (IGSCC) in chloride and caustic environments [17]. Failures due to

IGSCC have been experienced in the heat-Affected zone (HAZ) of type 316 SS welds exposed to marine environments due to sensitization and residual stresses introduced during welding [5]. Bouchard et al. in 2004 [33], suggested that the creep damage is due to creep cavities formation under a critical combination of stress, temperature and microstructure. This combination appears to be common in highly constrained welded components which may leads to restrain residual stresses. By detailed investigation of creep cavitation around a surface breaking crack within a stainless steel weld in an operating plant, they tried to predict the level of creep damage by existing empirical methods [34]. They found a model [35, 36],

aimed by finite element (FE) analysis to predict the welding residual stress by using, combined with an empirical multiaxial creep ductility model [37], which was able to capture the indispensable characteristics of the creep damage.

The cracking is caused by a combination of thermal relaxation of weld residual stress and limited material creep ductility at the performing temperature. At slower creep deformation rates, creep ductility decreases as occurred in plant operational conditions [38]. In another research by M.W. Spindler [37], it has been exhibited that, a highly tri-axial stress state which could be in certain weld types can largely diminish the creep ductility.

Turski *et al.* in 2008 [32], specially designed AISI Type 316 H austenitic stainless steel 25 mm thick compact tension specimens have been plastically deformed to produce significant tensile hydrostatic residual stresses at the notch root at mid-thickness. These specimens were thermally exposed at 550 °C for 4500 h to study the elevated-temperature creep relaxation of the residual stress and development of the reheat cracking creep damage. Residual strains within the specimens were measured using diffraction techniques before and after thermal exposure. A three-dimensional finite element model was developed both to predict the residual stress within the specimens before and after thermal exposure. No reheat cracking was found near surface, but due to the reduced creep ductility with increasing hydrostatic stress, noticeable creep cavitation was found mid-thickness. A previously developed creep damage model was applied to predict the onset of reheat cracking. Good correlation has been found between measurements and finite element predictions of strain and stress before and after thermal exposure. The extent of creep damage has also been assessed through destructive

examination, providing validation for the creep damage prediction model.

A subsequent ageing (at 550 °C for 4500 h) of the pre-conditioned fracture mechanics specimens resulted in observable creep damage [32, 39]. In contrast, in the Hossain research [40], the immediate exposure of quenched cylinders to ageing, again at 550 °C for about 4000 h did not result in the development of observable damage. Nevertheless, the predicted levels of creep damage via the same creep model, utilized in a FE code, indicated that the damage was similar to that seen in the fracture mechanics specimens and more widely spread. The contradictory results arising from these studies, suggest that the effects of pre-conditioning play a bigger role than expected and support the findings of Skelton *et al.* [41].

Hossain *et al.* [42, 43] utilized cylinders and spheres subjected to quenching. Rapid spray water quenching of the samples, initially at high temperature, induced tri-axial residual stresses in the center of the samples without the effects of prior plastic strain. A variety of techniques were then used to measure residual stresses in these studies. Turski *et al.* [32, 39], employed pre-compression to a fracture mechanics specimen and introduced a combination of residual stress and prior plastic strain around the crack tip in order to develop more uniform residual stress states in stainless steel samples. They employed both neutron and synchrotron diffraction methods to measure the residual stresses across the un-cracked section of the fracture mechanics specimen, while Hossain *et al.* [42, 43] limited their measurements in cylinders and spheres in order to comparison of the neutron diffraction measurements obtained from several laboratories. Measured residual stresses were found to compare reasonably well with predictions obtained from various FE simulations.

Hossain *et al.* in 2011 [1], investigated the creep residual stresses created in type 316 H stainless steel fracture mechanics specimens using the process of local out-of-plane compression (LOPC). Three sets of LOPC tools were employed to create different distributions of residual stress closely around the crack tip and the tools created different levels of prior plastic strain. Residual stresses were measured using the neutron diffraction method and compared with the stress predictions obtained from finite element (FE) simulations of LOPC. The specimens are then subjected to thermal exposure at 550 °C for several thousand hours. A creep deformation and damage model is introduced into the FE analysis to predict the relaxation of stresses and creation of damage in the specimens. Neutron diffraction experiments are undertaken to measure the relaxed residual stresses and fractographic analysis of thermally exposed samples measured the extent of creep damage. A comparison between measured and simulated results demonstrates that the prior plastic strain has a significant effect on damage accumulation but this is not accounted for in the current creep damage models.

As a matter of fact, creep does not only appear at high temperatures, but also occurs at low temperature for 316L stainless steel that menaces the equipment safety. In a research done by Li and Peng in 2019 [44], the creep behavior of as-received and pre-strained 316 L stainless steel at 373 K was investigated by uniaxial creep (UC) tests and small punch creep (SPC) tests. The parameters of power-law creep model were obtained by employing UC tests stress dependence. Afterwards, finite element (FE) simulation combined with power-law creep model was employed to analyze the creep behavior of SPC test. Comparing with experimental creep deflection, the results of FE simulation could reasonably reflect the creep behavior of as-received and pre-strained small

punch specimens. Based on the comparison of as-received specimen and pre-strained specimen from UC test, SPC test and FE simulation, pre-strain significantly restrains creep behavior of 316 L austenitic stainless steel at 373 K.

Effect of microstructure and cold work

Intergranular cracking can occur in heat-affected zones (HAZ) of austenitic stainless steel welded joints when reheated at the range of 500-700 °C. In this temperature range, residual stresses created during welding will be relaxed as a result of creep flow; however, the HAZ region may not sustain this small strain if its microstructure has been too severely altered during the welding which this may surpass the relaxation of such stresses, leading to initiation of cracks. This type of cracking, called reheat cracking, was originally identified in the 1950 s on Nb-stabilized austenitic stainless steel AISI 347 [45, 46].

The rate of stress corrosion cracking (SCC) was measured for non-sensitized, cold-worked Type 316 (UNS S31600) and Type 304 (UNS S30400) in both hydrogenated pressurized water and oxygenated water by Arioka *et al.* [47] in 2007. The stress dependence of 5% to 20% cold-worked Type 316 (CW316) was obtained in the PWR primary environment at 320°C. The rate of crack growth increased both with increasing cold work and stress intensity. Intergranular morphology was observed for 5%, 10%, 15%, and 20% CW316. Second, the dependence of crack growth rates from 250 °C to 320 °C were measured in both hydrogenated PWR primary and oxygenated water. More rapid crack growth rates were observed in oxygenated water than hydrogenated PWR water. The crack growth rates could be correlated with a $1/T$ dependence on temperature for both hydrogenated PWR primary and oxygenated water; apparent

activation energies of crack growth were similar in both environments. To assess what appeared to be common dependencies on temperature and cold work in both hydrogenated and oxygenated water, grain boundary creep (GB creep) was studied in air using CW316; intergranular creep cracking (IG creep cracking) was observed after low-temperature creep tests in air. The noticeable activation energy of IG creep cracking was similar to that of intergranular stress corrosion cracking (IGSCC) in high temperature water which these results illustrate the important role of GB creep. Ni enrichment, Fe, and Cr depletion was observed at the grain boundary ahead of the IG creep crack tip. This result supported the GB diffusion occurrence before crack progress and it can be concluded that critical process in IG creep cracking and IGSCC is diffusion of vacancies at the grain boundary. The similar dependencies on temperature, cold work, and rolling direction of SCC and creep suggests the grain boundary diffusion creep as a critical role in the growth of SCC.

Kim *et al.* in 2019 [48], investigated the high-temperature creep behavior of gamma Ti-48Al-2Cr-2Nb alloy additively manufactured by electron beam melting. Due to lower cooling rate of Electron beam melting (EBM) than other additive manufacturing processes such as selective laser melting, laser metal deposition, etc., makes it suitable for fabricating titanium aluminide-based intermetallic. A gamma Ti-48Al-2Cr-2Nb alloy was manufactured using EBM, and its microstructure and high-temperature creep behaviors were investigated. EBM-built Ti-48Al-2Cr-2Nb alloy had a near-gamma (NG) structure confirmed by initial microstructural observation, whereas the conventional Ti-48Al-2Cr-2Nb alloy had a fully lamellar (FL) structure. The Ti-48Al-2Cr-2Nb alloy with the NG structure had lower strength in all temperature ranges, and the yield-

strength anomaly phenomenon occurred in both materials confirmed by room temperature and high temperature compression tests. A multi-step creep test applied at 750 °C confirmed that the EBM-built Ti-48Al-2Cr-2Nb alloy with lower strength had lower creep resistance as well. Microstructural observation after creep deformation confirmed that mechanical twins and dislocation movement were been dominantly formed in the material creep deformation with the NG structure. In the FL structure, diffusional creep in low-stress regions and huge deformation at the colony boundary in high-stress regions dominated the creep deformation.

Creep-fatigue combination behavior

The 316 stainless steels may be operated at high temperature environments with high gradients, as those occurring in aircraft gas turbine engine or hot section combustor liners. In addition to low cycle fatigue (LCF) damages due to the startup/shut-down cycling, the high-temperature components are exposed to the time-dependent creep damage due to their normal operation at elevated temperatures during services [4]. In a gas turbine of an airplane that is subjected to take-off, considering the discs and blades, steady-state cruising, and a short landing, during the on-load cruising periods many time-dependent factors can be take placed which creep is the most important factor. The similar behaviors are observed in many other systems such as pressure vessels and heat exchangers. Therefore, the stress-strain behavior of the components under cyclic loading and both creep-fatigue damages when characterizing the mechanical behaviors need to be utterly perceived [4]. Also, type 316 SS materials are subject to cyclic strains that are produced thermally and/or mechanically and under these constant and cyclic temperatures, isothermal

and thermo-mechanical fatigue (TMF) damages occur which will lead to the initiation of cracking and subsequent crack growth [14].

Srinivasan *et al.* in 2003 [13], studied the (LCF) behavior of solutionized 316 L (N) stainless steel (SS) at various temperatures, strain amplitudes, strain rates, hold times and in 20% prior cold worked condition. In general, the alloy exhibited a deduction in fatigue life with temperature rising, strain rate reduction, increase in strain amplitude, duration of hold time in tension and with prior cold work. The LCF and creep-fatigue interaction (CFI) behavior of the alloy was explained on the basis of several operative mechanisms such as dynamic strain ageing, creep, oxidation and sub structural recovery. Artificial neural network (ANN) capability was evaluated approach to life prediction under LCF and CFI conditions by using the data generated. ANN approach led to LCF and creep-fatigue life prediction within a factor of 2 and in most cases within a factor of 1.5. Prediction was very close to the actual lives for some data points. The life prediction for a wide variety of testing conditions was successful as sufficient care was taken over selection of input variables, data normalization and transformation of input variables apart from applying optimum values of ANN parameters.

Hormozi *et al.* in 2015 [14], applied a detailed investigation of low cycle fatigue (LCF) and thermos-mechanical fatigue (TMF) of a 316FR stainless steel in order to recognize the failure mechanism based on experimental results and the following samples metallography. The material used was a type 316 FR stainless steel, similar to type 316 L (N). Type 316 FR is a low-carbon grade of stainless steel with a more closely specified nitrogen content and chemistry modified to increase high-temperature performance. The LCF-TMF servohydraulic testing with a temperature

consistency of less than ± 5 °C within the gauge section of the specimens was employed to perform the experimental tests. Fully-reversed, strain-controlled isothermal tests were applied at 650 °C for the strain ranges of $\Delta\varepsilon = \pm 0.4\%$, $\pm 0.8\%$, $\pm 1.0\%$ and $\pm 1.2\%$. Strain-controlled in-phase (IP) thermo-mechanical fatigue tests were conducted on the same material and the temperature was cycled between 500 °C and 650 °C. Furthermore, the creep-fatigue influence was investigated through the symmetrical hold time under both LCF-TMF tests.

Hormozi *et al.* in 2015 [4], following of their previous work [14], proposed a constitutive model based on the isotropic and nonlinear kinematic hardening rules to replicate the numerically the cyclic structural behavior of the material until stabilization. The creep-fatigue behavior of the 316 FR material was conducted through experimental tests and numerical analysis. Experimental tests were conducted in order to investigate and analyze the experimental stress-strain data for the LCF tests under strain-controlled condition with and without hold time at the temperature of 650 °C. Numerical analysis of the material behavior for the three stages of cyclic hardening, stabilization and failure for the LCF tests conducted under strain-controlled condition with and without hold time at 650 °C was analyzed and reproduced. In order to demonstrate the damage initiation and the damage evolution, a hysteresis energy-based phenomenological model (for the tests with continuous cyclic loading) was carried out in a user subroutine combined with a creep damage model based on the time-fraction law to reproduce the experimental results. Table 4 shows the research works studied variant factors influence on creep behavior of 316 austenitic stainless steel.

Table 4. Effect of variant factors on creep behavior on 316 austenitic stainless steel in literature.

Material	Identifying factor influencing on creep behavior	year	Ref.
316, 316LN	Influence of carbon and nitrogen	1991	[17]
316L, 316LN	Alloying nitrogen	2000, 2012, 2009	[5, 15, 16]
316L	Alloying N and Cu	2016	[31]
316H	Creep cavitation in a pressure vessel	2004	[33]
304, 316	Cold Work, temperature and microstructure effect on creep	2016, 2007	[6, 47]
316H, 316 L	Residual stress	2008, 2006, 2007	[32, 42, 43]
316H, 316L	Residual stress and plastic strain	2004, 2011, 2019	[1, 33, 44]
316, 316L, 316 LN, 316 FR	Creep-fatigue behavior	2015, 2016, 2007	[2, 6, 13]
316 FR	LCF/TMF influence on creep-fatigue behavior	2015	[4, 14]

Conclusions

This review discussed the creep behavior the of 316 austenitic stainless steel and some identifying factors such as addition of N and Cu into the matrix, residual stress and pre-strain, microstructure and cold work, and the creep-fatigue combination behavior on 316 steel are discussed. It was found that, nitrogen can improve the creep and fatigue strength at high temperatures and fracture toughness at low temperatures. The addition of N was found to be beneficial to creep properties at all the stress levels and creep rupture strength increased substantially with increase in N content leads to enhance the creep rupture life. The addition of copper can improve the creep life at low stress, due to the fine precipitation of the Cu-rich phase. While the formation of copper-rich phase before the failure does not influence the creep life under high stress. The creep rupture can be due to creep cavities formation under a critical combination of stress, temperature and microstructure. This combination prevalently appears in highly constrained welded components which may leads to restrain residual stresses. Also, prior pre-strain especially closely around the crack tip and created at different levels of prior plastic strain

can lead to creep damage and severe the conditions with combination of residual stresses. Microstructure and cold work play an important role on creep mechanism and behavior. Creep diffusion mechanisms highly rely on the type of microstructure, grain boundaries and cold work levels employed. Creep-fatigue combination behavior was also discussed. Cyclic strains which are thermally and/or mechanically generated under constant and cyclic temperatures, isothermal and thermo-mechanical fatigue (TMF), may lead to initiation of cracking and subsequent crack growth in type 316 stainless steels.

Disclosure Statement

No potential conflict of interest was reported by the authors.

Orcid

Mohammad Sajjadnejad  0000-0001-5112-1791

References

- [1]. Hossain S., Truman C.E., Smith D. *J. Fatigue Fract. Eng. Mater. Struct.*, 2011, **34**:654

- [2]. Yan X.L., Zhang X.C., Tu S.T., Mannan S.L. Xuan F.Z., Lin Y.C., *Int. J. Pres. Ves. Pip.*, 2015, **126**:17
- [3]. Coleman M., Miller D., Stevens R., Integrity of High-Temperature Welds, Conference, Nottingham, November, Professional Engineering Publishing Ltd., Bury St Edmunds, IP32 6BW, UK. 1998
- [4]. Hormozi R., Biglari F., Nikbin K. *Eng. Fract. Mech.*, 2015, **141**:19
- [5]. Sasikala G., Mannan, S.L., Mathew M.D., Bhanu Rao K. *Metall. Mater. Trans.*, 2000, **31**:1175
- [6]. Ghosh A., Gurao N., *Mater. Des.*, 2016, **109**:186
- [7]. Plaut R.L., Herrera C., Escriba D.M., Rios P.R., Padilha A. F. *Mat. Res.*, 2007, **10**:453
- [8]. Viswanathan R., *Damage mechanisms and life assessment of high temperature components; ASM international*: 1989; p 1-440
- [9]. Maruyama K., Baba, E., Yokokawa K. *Tetsu-to-Hagane*, 1994, **80**:336
- [10]. Spindler M.W., Spindler S.L. *Int. J. Pres. Ves. Pip.*, 2008, **85**:89
- [11]. Holmström S., Auerkari P. *Materials at High Temperatures*, 2008, **25**:103
- [12]. Maruyama K., Armaki H.G., Yoshimi K. *Int. J. Pres. Ves. Pip.*, 2007, **84**:171
- [13]. Srinivasan V., Valsan M., Bhanu Sankara Rao K., Mannan S.L., *Raj B. Int. J. Fatigue.*, 2003, **25**:1327
- [14]. Hormozi R., Biglari F., Nikbin K. *Int. J. Fatigue.*, 2015, **75**:153
- [15]. Mathew M.D., Laha K., *Ganesan. V. Mater. Sci. Eng. A.*, 2012, **535**:76
- [16]. Ganesan V., Mathew M.D., Sankara Rao K.B. *Mater. Sci. Tech-Lond*, 2009, **25**:614
- [17]. Mathew M.D., Sasikala G., Bhanu Sankara Rao K., Mannan S.L. *Mater. Sci. Eng. A.*, 1991, **148**:253
- [18]. Stoltz R., *Vander Sande J. Metall. Mater. Trans.*, 1980, **11**:1033
- [19]. Lee H.J., Lee C.S., Chang Y.W. *Metall. Mater. Trans.*, 2005, **36**:967
- [20]. Degallaix S., Foct S.J., Hendry A.J. *Mater. Sci. Technol.*, 1986, **2**:946
- [21]. Müllner P., Solenthaler C., Uggowitzer P., Speidel M.O. *Fundamental Aspects of Dislocation Interactions; Institute of Metallurgy, ETH Zürich (Switzerland)*: 1993; p 164-169
- [22]. Mathew M.D., Kumar J.G., Ganesan V., Laha K. *Metall. Mater. Trans.*, 2014, **45**:731
- [23]. Chi C.Y., Yu H.Y., Dong J.X., Liu W.Q., Cheng S.C., Liu Z.D., Xie Z.S. *Pro. Nat. Sci-Mater.*, 2012, **22**:175
- [24]. Bai J.W., Liu P.P., Zhu Y.M., Li X.M., Chi C.Y., Yu H.Y., Xie X.S., Zhan Q. *Mater. Sci. Eng. A*, 2013, **584**:57
- [25]. Zhang Y., Wang L., Jiang W., Bai G., Chen L. *Mater. Trans.*, 2005, **46**:2015
- [26]. Sen I., Amankwah. E., Kumar N.S., Fleury, E., Oh-ishy K., Hono K., Ramamurty U. *Mater. Sci. Eng. A*, 2011, **528**:4491
- [27]. He S.M., Van Dijk N.H., Paladugu M., Schut H., Kohlbrecher J., Tichelaar F.D., Van der Zwaag S. *Phys. Rev. B*, 2010, **82**:174111
- [28]. Zhang S., Schut H., Bruck E., Van der Zwaag S., Van Dijk N.H. *Journal of Physics: Conference Series 443*, IOP Publishing, 2013
- [29]. Zhang S., Schut H., Kohlbrecger J., Langelaan G., Bruck E., Van der Zwaag S., Van Dijk N.H. *Philos. Mag*, 2013, **93**:4182
- [30]. Laha K., Kyono J., Shinya N. *Scr. Mater.*, 2007, **56**:915
- [31]. Cai B., Kang J.H., Hong C.W., Kim S.J. *Mater. Sci. Eng. A*, 2016, **662**:198
- [32]. Turski M., Bouchard P.J., Steuwer A., Withers P.J. *Acta Mater*, 2008, **56**:3598
- [33]. Bouchard P.J., Withers P.J., McDonald S.A., Heenan R.K. *Acta Mater*, 2004, **52**:23
- [34]. *Energy B. Assessment procedure for the high temperature response of structures: British Energy Generation Limited; Document R5, 2003; Paper ID 458.*
- [35]. Holt P., Spindler M.W. *A practical application of continuum damage mechanics to*

plant integrity assessment, *Proceedings of the Symposium on Elasticity and Damage in Solids Subject to Microstructural Change*, Newfoundland. 1996

[36]. Bradford R.A.W. Finite Element Modelling of Reheat Cracking Initiation in Austenitic Weldments, *Institute of Mechanical Engineers Conference Transactions, International Conference on "Assuring It's Safe"*, 18-19 May 1998, Heriot-Watt University, Edinburgh, UK, paper C535/023/98, pp 287-295

[37]. Spindler M. *Fatigue Fract. Eng. Mater. Struct.*, 2004, **27**:273

[38]. Hales R. *Fatigue & Fracture of Engineering Materials & Structures*, 1983, **6**:121

[39]. Turski M., Sherry A.H., Bouchard P.J., Withers P.J. *J. Neutron Res.*, 2004, **12**:45

[40]. Hossain S. *Residual stresses under conditions of high triaxiality*, University of Bristol.

[41]. Skelton R.P., Goodall I.W., Webster G.A., Spindler M.W. *Int. J. Pres. Ves. Pip.*, 2003, **80**:441

[42]. Hossain S., Truman C.E, Smith D.J., Daymond M.R. *Int. J. Mech. Sci.*, 2006, **48**:235

[43]. Hossain S., Truman C.E, Smith D.J., Peng R.L, Stuhr U. *Int. J. Solids Struct.*, 2007, **44**:3004

[44]. Li K.S., Peng J., *Key Engineering Materials*, 2019, **795**:152

[45]. Emerson R.W., Jackson R.W., Dauber C.A. *Welding J.*, 1962, **41**:385

[46]. Curran R.M., Rankin A.W., *Weld. J.*, 1955, **34**:205

[47]. Arioka K., Yamada T., Terachi T., Chiba G. *Corrosion*, 2007, **63**:1114

[48]. Kim Y.K., Youn S.J., Kim S.W., Hong J., Lee K.A. *Mater. Sci. Eng. C.*, 2019, **763**:138138

How to cite this manuscript: Mohammad Sajjadnejad*, Seyyed Mohammad Saleh Haghshenas, Mina Tavangar, Niloofar Ghani Kolahloo. Creep behavior of 316 austenitic stainless steel under variant operating conditions. *Asian Journal of Nanoscience and Materials*, 3(4) 2020, 266-279. DOI: 10.26655/AJNANOMAT.2020.4.1